Available online at www.sciencedirect.com
SCIENCE DIRECT®
Experimental Cell Research 293 (2004) 331–345
Experimental Cell Research
www.elsevier.com/locate/yexcr

The interferon-inducible IFI16 gene inhibits tube morphogenesis and proliferation of primary, but not HPV16 E6/E7-immortalized human endothelial cells

Ravera Raffaella,[a] Daniela Gioia,[b] Marco De Andrea,[a] Paola Cappello,[c] Mirella Giovarelli,[c] Peggy Marconi,[d] Roberto Manservigi,[d] Marisa Gariglio,[b] and Santo Landolfo[a,*]

[a] *Department of Public Health and Microbiology, University of Turin, 10126 Turin, Italy*
[b] *Department of Medical Sciences, University of Eastern Piedmont, Novara, Italy*
[c] *CERMS, San Giovanni Battista Hospital, Turin, Italy*
[d] *Department of Experimental and Diagnostic Medicine, University of Ferrara, Ferrara, Italy*

Received 31 July 2003, revised version received 17 October 2003

Abstract

Immunohistochemical analysis has demonstrated that the human IFI16 gene, in addition to the hematopoietic tissues, is highly expressed in endothelial cells and squamous stratified epithelia. In this study, we have developed a reliable HSV-derived replication-defective vector (TO-IFI16) to efficiently transduce IFI16 into primary human umbilical vein endothelial cells (HUVEC), which are usually poorly transfectable. HUVEC infection with TO-IFI16 virus suppressed endothelial migration, invasion and formation of capillary-like structures in vitro. In parallel, sustained IFI16 expression inhibited HUVEC cell cycle progression, accompanied by significant induction of p53, p21, and hypophosphorylated pRb. Further support for the involvement of these pathways in IFI16 activity came from the finding that infection with TO-IFI16 virus does not impair the in vitro angiogenic activity and cell cycle progression of HUVEC immortalized by HPV16 E6/E7 oncogenes, which are known to inactivate both p53 and pRb systems. This use of a reliable viral system for gene delivery into primary human endothelial cells assigns a potent angiostatic activity to an IFN-inducible gene, namely IFI16, and thus throws further light on antiangiogenic therapy employing IFNs.

Keywords: IFN-inducible IFI16 gene; HUVEC; Tube morphogenesis; Cell growth arrest; HPV16 E6/E7; p53; pRb

Introduction

Angiogenesis is mediated by multiple positive and negative regulatory molecules: the balance of these mediators determines the outcome of this process [1,2]. Anti-angiogenic therapy uses negative neovascularization regulators to suppress pro-angiogenic signals or increase inhibitory signals [3]. IFNs, along with their role in viral interference and cell proliferation, possess potent antiangiogenic activity [4–6]. They down-regulate the expression of several proangiogenic molecules, such as bFGF [7], matrix metalloproteases (MMP-2 and MMP-9) [8–10], and IL-8 [11].

Binding of IFNs to their cognate cell surface receptors initiates a series of intracellular signaling cascades resulting in the activation of specific target genes, known as IFN-stimulated genes (ISGs) [12]. The proteins encoded by these genes mediate the necessary biological response [12]. Hundreds of cellular genes can be induced following IFN stimulation, whereas the molecular and biological functions of many of their products are often not known. Among these are the members of the Ifi200 family in mice (Ifi202, Ifi204, Ifi203, and D3) [13–15] and their human counterpart (HIN200 family), including IFI16 [16], MNDA (Myeloid Nuclear Differentiation Antigen) [17], and AIM2 (Absent In

Abbreviations: AIM2, absent in melanoma 2; bFGF, basic fibroblast growth factor; HSV, herpes simplex virus; hEGF, human epidermal growth factor; HUVEC, human umbilical vein endothelial cells; IFNs, interferons; IGF-1, insulin growth factor-1; ISGs, IFN-stimulated genes; MNDA, myeloid nuclear differentiation antigen; moi, multiplicity of infection; VEGF, vascular endothelial growth factor.

* Corresponding author. Department of Public Health and Microbiology, University of Turin, Via Santena 9, 10126 Turin, Italy. Fax: +39-11-6966977.
E-mail address: santo.landolfo@unito.it (S. Landolfo).

0014-4827/$ - see front matter © 2003 Elsevier Inc. All rights reserved.
doi:10.1016/j.yexcr.2003.10.014

Melanoma 2) [18]. A highly conserved 200-amino-acid domain present singly or in duplicate is a structural motif found in all members and harbors an LXCXE motif that is a potential site for binding to the retinoblastoma gene products [13–15].

Several reports have examined the molecular and cellular functions of mouse Ifi200 and human HIN-200 proteins. Overexpression of p204 in mouse embryo fibroblasts retarded their proliferation, delayed G1 progression into S-phase, and accumulated cells with a DNA content equivalent to cells arrested in late G1 [19]. These effects were strictly dependent on the association of progression with the Rb proteins [20,21]. Sustained expression of p204 induced the fusion of C2C12 myoblasts to myotubes, suggesting that it may be involved in muscle differentiation [22]. In humans, Johnstone et al. [23] demonstrated that IFI16 and p53 interact in vitro and in vivo to cause a dose-dependent increase in p53-mediated transactivation. A correlation between binding of IFI16 to p53 and modulation of p53-mediated transactivation was also observed. However, the physiological significance of the IFI16/p53 interaction and the precise mechanism(s) involved in the regulatory function of IFI16 on p53 still need to be fully dissected.

Consistent with a role for p200-family proteins in cell-growth regulation, there are indications that viral oncoproteins functionally inactivate p202 [24]. Expression of AIM2 is lost by frameshift mutations in colorectal tumors, and loss of MNDA expression in prostate carcinoma is linked to progression to more aggressive metastatic prostate cancer [25,26]. Recent studies have revealed that increased levels of IFI16 in prostate epithelial cells contribute to senescence-associated irreversible cell growth arrest. Moreover, its overexpression in human prostate cancer cell lines, which did not express IFI16, inhibited colony formation [27]. Altogether, these observations support the idea that the loss of function of p200-family proteins, by providing growth advantage to the affected cells, may contribute to the development of cancer.

Previous immunohistochemical analysis has demonstrated strong IFI16 expression in lymphocytes and monocytes [16]. By contrast, only some resident macrophages were stained and granulocytes were negative. In addition, in normal adult human tissues, IFI16 is expressed in a highly restricted pattern in selected cells within certain organs [28,29]. Prominent IFI16 expression is seen in stratified squamous epithelia, particularly intense in basal cells in the proliferating compartments, whereas it gradually decreases in the more differentiated suprabasal compartment. In addition, all vascular endothelial cells from both blood and lymph vessels strongly expressed IFI16.

As IFI16 modulates transcriptional activation by p53 and regulate the cell cycle through interaction with pRb, and since it is highly expressed in endothelial cells, it is conceivable to infer that IFI16 regulates endothelial cell physiology through these mechanisms.

In this study, we have developed a reliable HSV-derived replication-defective vector [30,31] to efficiently transduce IFI16 into primary human umbilical vein embryo cells (HUVEC), which are usually poorly transfectable by conventional methods. Evaluation of some features of in vitro angiogenesis, namely chemotaxis, Matrigel invasion, tube morphogenesis, and cell cycle progression, has provided for the first time demonstration that the IFN-inducible protein IFI16 impairs the tube morphogenesis and proliferation of human endothelial cells. The observation that HPV16 E6/E7 oncogenes abolish this activity suggests that IFI16 directly acts on the tubulogenesis and proliferation of primary HUVEC through the interaction with p53 and/or pRb pathways.

Materials and methods

Isolation and culture of HUVECs

HUVEC were isolated from cannulated human umbilical veins by treatment with collagenase and maintained in complete endothelial growth medium (EGM-2, Clonetics, San Diego, CA) containing 2% FBS, human recombinant vascular endothelial growth factor (VEGF), basic fibroblast growth factor (bFGF), human epidermal growth factor (hEGF), insulin growth factor (IGF-1), hydrocortisone, ascorbic acid, heparin, GA-1000 (gentamicin and amphotericin B, 1 μg/ml), according to the recommendations of the supplier. Each culture was used only up to five population doublings. The cells were seeded into 100-mm culture dish coated with 0.2% gelatin and grown under 5% CO_2 at 37°C in medium renewed every 3–4 days. When indicated, HUVEC were growth-arrested by confluence and culturing them for 48 h in basal EBM-2 medium containing 2% FBS and supplements, but lacking VEGF, bFGF, hEGF, and IGF-1.

Plasmid and recombinant virus constructions

Plasmids are pUL41-ICPO-lacZ and pUL41-ICPO-IFI16. The reporter construct consisted of the lacZ gene upstream from the SV40 polyadenylation signal flanked by *Pac*I restriction sites [30,31]. In the plasmid, the reporter gene, under the control of the herpes ICP0 promoter, was placed within the UL41 coding sequences to allow homologous recombination of the expression cassette into the viral genome. The full-length IFI16 cDNA (Asp718 2700-bp fragment from pBKS-IFI16; kindly provided by Joseph Trapani) was placed downstream from the ICP0 promoter after digestion with *Eco*RI and *Xba*I blunt-ended to remove the lacZ gene. The vector TOZ was created by recombining the lacZ expression cassette described above into the UL41 locus of the replication defective herpes mutant deleted of ICP4, ICP27, and ICP22 IE genes (T.2), and therefore incapable of replicating in cells that do not express the essential ICP4 and ICP27 genes in trans. Briefly, T.2 genome DNA was cotransfected with 1 μg linearized

pUL41-ICP0-lacZ plasmid, containing the lacZ gene flanked by the unique *Pac*I sites within the UL41 viral sequences, using the $CaPO_4$ method into monolayers of 7B cells in 60-mm culture plates. Recombinant viruses created by disruption of UL41 and its replacement by the lacZ expression cassette were identified by their blue plaque phenotype after X-gal staining. The vector TO-IFI16 was generated by homologous recombination between TOZ viral DNA and the plasmid pUL41-ICP0-IFI16 using the *Pac*I recombination system as described above. Recombinants containing IFI16 in place of the lacZ reporter gene were identified by their clear plaque phenotype after X-gal staining. Recombinant viruses form individual plaques were purified to homogeneity by three rounds of limiting dilution, and the presence of the transgene in place of lacZ was identified by Southern blot analysis. Titers of all stocks were determined by plaque formation in the complementing cell line 7B with agar overlay as described by Marconi et al. [31].

Recombinant herpes virus infection

HUVECs were infected in suspension with TOZ and TO-IFI16 at a concentration of 1×10^6 plaques forming units (p.f.u.)/ml in EGM-2 medium with 0.5% FBS, for 90 min at 37°C at moi 2. The infected cells were then seeded in 60-mm culture dishes in EGM-2 medium with 2% FBS. After 6 h, the medium was discarded, and the cells were extensively washed and cultured in fresh medium with 2% FBS. To measure the efficiency of infection after 24-h incubation, β-galactosidase was evaluated using X-gal as substrate.

Retroviral expression vectors

The retroviral vector pBabe-puro containing the HPV16 E6/E7 ORF was kindly provided by Massimo Tommasino (International Agency for Research on Cancer, Lyon, France). High-titer retrovirus-containing supernatants (>5×10^6 IU/ml) were generated by transient transfection of second-generation retrovirus producer Phoenix cells and used to infect the cells as previously described by Pear et al. [32]. After infection, HUVEC were selected in 0.2 μg/ml puromycin for 10 days and designated E6/E7 HUVEC.

Western blot analysis

For crude extract preparation, cells were lysed in 3% SDS-lysis buffer containing 125 mM Tris–HCl pH 6.8, 3% SDS, 10 mM DTT, 10% glycerol with the addition of protease inhibitors (0.2 mM PMSF, 1 mg/ml pepstatin, 0.1 mM benzamidine, 2 mg/ml aprotinin), and briefly sonicated [16]. Insoluble material was removed by centrifugation at 13,000 rpm for 5 min. Protein concentration was determined by the Bio-Rad D_c Protein Assay (Bio-Rad Laboratories). Proteins were separated on an 8.5% or 15% SDS-polyacrylamide gel and transferred onto a PVDF membrane (Amersham) according to the instruction manual. The membrane was blocked in a blocking solution (10 mM Tris–HCl pH 7.5, 0.1 M NaCl, 0.1% Tween-20, 5% [w/v] nonfat dry milk) overnight at 4°C, and incubated with affinity-purified anti-IFI16 rabbit polyclonal antibody (diluted 1:2000), pRb, p53, and p21WAF1 (all from Santa Cruz Biotechnology), pRb Ser780 (Cell Signaling Technology), actin (Chemicon International). Appropriate secondary Abs conjugated with horseradish peroxidase conjugate were used (Sigma), and the chemiluminescence reaction was visualized by enhance chemiluminescence (Pierce Supersignal), according to the manufacturer's instructions. Densitometry was performed by scanning the radiographs and then analyzing the bands with Quantity One software (Bio-Rad).

Chemotaxis assays

This test was carried out in Boyden chambers as described by Albini et al. [33]. Briefly, uninfected or infected HUVEC were resuspended in EBM2 with 0.1% BSA. The lower compartment of Boyden chambers was filled with 200 μl EGM2 containing VEGF and bFGF as chemoattractants. EBM-2 without chemoattractants added of 0.1% BSA was used as a negative control. HUVEC (1×10^5/400 μl/chamber) were placed in the upper compartment. The two compartments were separated by a polycarbonate filter (12-μm pore size) coated with gelatin (5 mg/l) to allow cell adhesion. The chambers were incubated for 6 h at 37°C in a humidified atmosphere containing 5% CO_2. After incubation, cells on the upper side of the filter were removed. The cells that had migrated to the lower side of the filter were fixed in 3% paraformaldeyde, washed in PBS, and stained with crystal violet. Eight to ten units/field per filter were counted at ×160 magnification with a microscope (Olympus).

Chemoinvasion assay

The invasion assays were carried out as described for the chemotaxis assays with the following modifications. The filter insets (upper chambers) were coated with growth factor-depleted Matrigel (1 mg/ml), a reconstituted basement membrane. This assay assesses the invasive capability of endothelial cells by mimicking the process of extravasation through the vascular basement membrane [34].

Matrigel morphogenesis assay (tube morphogenesis)

A 24-microwell plate, prechilled at −20°C, was coated with 300 μl/well of Matrigel Basement Membrane (5 mg/ml; Becton and Dickinson) and then placed in an incubator at 37°C for 30 min until solidified. HUVEC in complete medium, either uninfected or infected [8×10^4 cells/(500 μl well)], were seeded onto the matrix and allowed to incubate at 37°C in a 5% CO_2 environment. Plates were photographed at 12 h using an Olympus inverted microscope.

Cell cycle analysis

Cell cycle analysis was performed using the PI staining of DNA. Briefly, cells were harvested and fixed in 50% cold ethanol for 60 min at 4 °C. The cells were then washed twice with PBS, incubated at 37 °C in citrate buffer (0.05 M Na_2HPO_4, 25 mM sodium citrate, 0.1% Triton X-100 pH 7.8), and stained with 100 μg/ml PI for 30 min (for dye stabilization) in the presence of RNase (100 ng/ml). Cellular DNA content was then assessed with a FACScalibur flow cytometer (Becton and Dickinson) and analyzed with the ModFit LT software program (Becton and Dickinson).

Results

Modulation of IFI16 expression during endothelial cell growth

Immunohistochemical analysis demonstrated that IFI16 is highly expressed in endothelial cells, suggesting that it may be involved in angiogenesis [28,29]. When HUVEC are maintained at subconfluent density in complete medium, they proliferate and are highly sensitive to growth arrest by contact inhibition. A representative cell cycle profile for proliferating or growth-arrested HUVEC is presented in Fig. 1A. Typically, 43.5% of proliferating cells are in G1, 35.8% in S, and 20.7% in G2. Confluence is followed by growth arrest with more than 70% of cells in G1, 11.9% in S phase, and 16.4% in G2. To define the optimal culture conditions for infection with transducing viral vectors, HUVEC were seeded at different cell concentration/cm^2 (from 2.5×10^3 to 1.5×10^4 cells) and after 48 h, cell extracts were analyzed for IFI16 expression by Western blotting analysis. As shown in Fig. 1B, in proliferating cells with the majority of the cells in S and G2/M phases, IFI16 was barely detectable (lane 1). By contrast, upon reaching confluence-induced growth arrest, significantly higher levels of all three IFI16 protein isoforms were observed (lanes 2 and 3).

Altogether, these results demonstrate that proliferating HUVEC express low levels of endogenous IFI16 protein

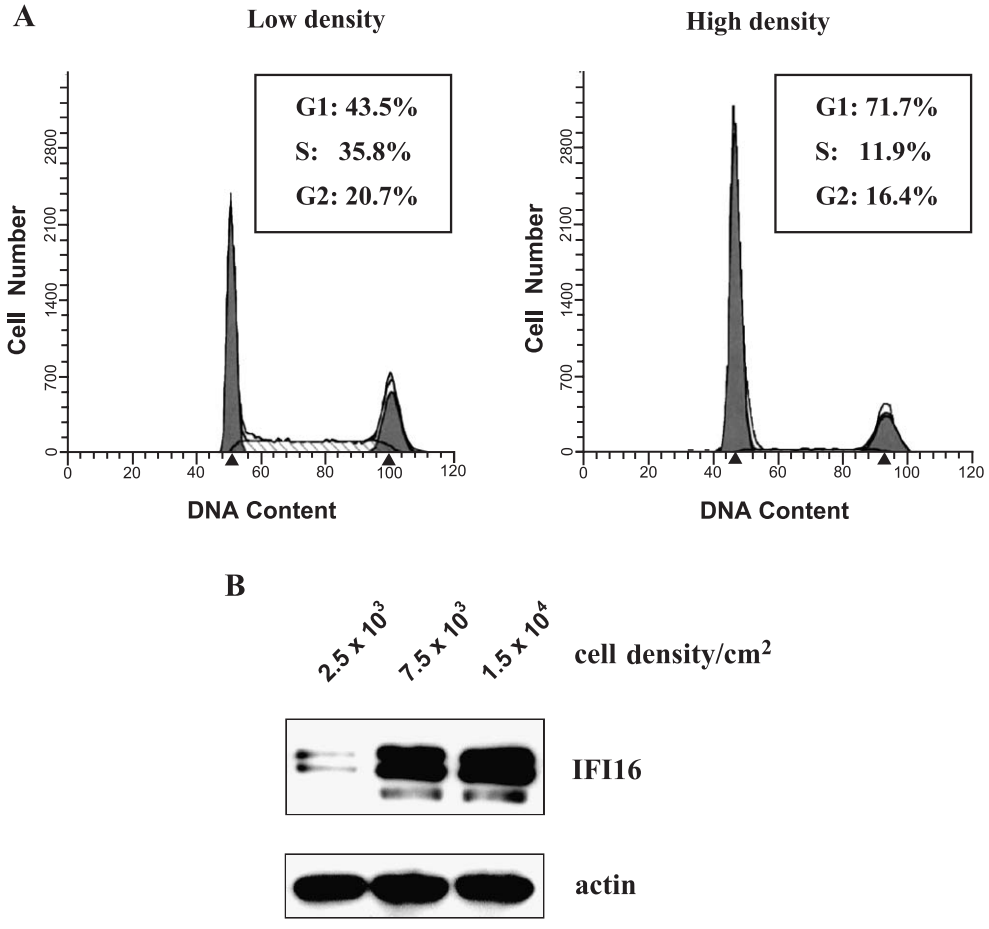

Fig. 1. Expression of IFI16 protein in HUVEC proliferating or growth-arrested by contact inhibition. (A) Cell cycle distribution of HUVEC cultured at low (2.5×10^3/cm^2) or high (1.5×10^4/cm^2) density as measured by DNA content flow cytometry. The experiment has been repeated three times and one representative is reported. (B) HUVEC were cultured at increasing cell densities per cm^2 (2.5×10^3, 7.5×10^3, 1.5×10^4 cells, respectively), and after 48 h, total cell lysates were analyzed in immunoblots with anti-IFI16 affinity-purified rabbit polyclonal monospecific Abs. Actin immunodetection with a monoclonal antibody (Chemicon International) was performed as internal control.

and therefore represent a suitable system for infection with the HSV-derived vectors.

Construction of a replication-defective herpes simplex virus vector for efficient IFI16 transduction in HUVEC

The triply-deleted replication-defective herpes simplex virus (HSV) T.2, in which the ICP4, ICP27, and ICP22 genes have been deleted, shows substantially reduced cytotoxicity and can be used to efficiently transfer and transiently express transgenes in many cell types. The vector TO-IFI16 was created in two steps. First, the bacterial lacZ gene, under the control of the HSV ICP0 IE promoter and flanked by *Pac*I restriction sites (not present in the viral genome), was inserted into the UL41 locus of the replication-deficient vector T.2, to generate TOZ, as illustrated in Fig. 2A. Subsequently, using the *Pac*I system (see Materials and methods), the transgene was introduced into the UL41 locus of TOZ vector by digestion of the viral DNA and by homologous recombination with an expression cassette containing the cDNA encoding IFI16 (isoform B) under the control of the HSV ICPO IE promoter. This promoter has been previously shown to express transgenes efficiently. A herpesvirus vector expressing the β-galactosidase as reporter gene, termed TOZ, was used to evaluate the efficiency of gene delivery to the endothelial cells.

To evaluate whether HUVEC infected with TO-IFI16 recombinant virus could express IFI16 and to quantify the transgene levels, Western blotting assay was performed on total proteins extracted from cells infected at different time points at a multiplicity of infection (moi) of 2. This moi was chosen because when the TOZ recombinant virus was used, it yielded more than 80% of blue cells after X-gal staining (data not shown). In accord with previous reports [31], we also observed increases in IFI16 isoform B steady state levels in TO-IFI16-infected cells. Its levels peaked between 24 h and 48 hpi (Fig. 2B, lanes 3 and 5), and then gradually declined, being substituted by the increase of the endogenous IFI16 isoforms (Fig. 2B, lanes 6 and 7). By contrast, in TOZ-infected cells, IFI16 was barely detectable at 24 hpi when cells proliferate vigorously and significantly increased at 72 hpi when cells cease to grow because of contact inhibition. This expression pattern is in line with earlier reports showing that transgene expression in HSV replication defective vectors peaks in the first 24–48 hpi and gradually decreases in the next few days [31].

By using the highly efficient infection conditions described above, we then determined whether IFI16 overexpression affects the in vivo growth kinetics of HUVEC. The cell growth number was assessed at 24 h periods over 96 h. After the indicated hours, cells were detached and counted by Trypan blue assay as previously described [20]. As shown in Fig. 2C, the growth kinetics of TOZ-infected cells was similar to the uninfected cells: the cell number doubled every 24 h and peaked at 72 h after cell seeding. Interestingly, the number of TO-IFI16-infected HUVEC did not vary significantly in the first 48 h when the levels of exogenous IFI16 are maximal, and started to double after 72 h along with the decrease of exogenous IFI16 expression. Moreover, the slope of the growth curve demonstrates that sustained and transient expression of exogenous IFI16

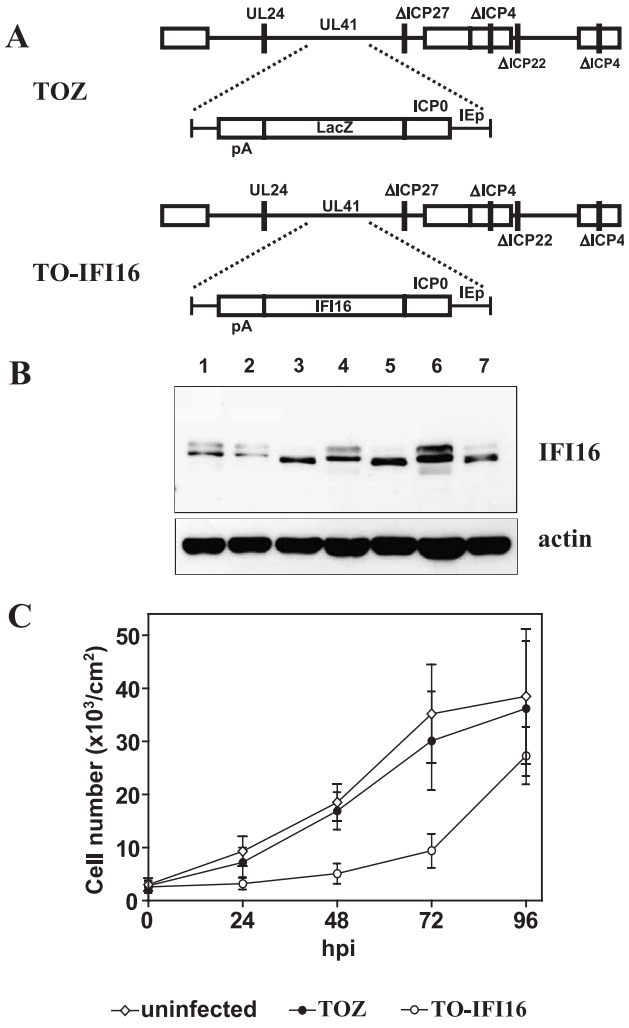

Fig. 2. HSV-transduced IFI16 expression is inversely related to endothelial cell proliferation. (A) Schematic representation of the recombinant vectors TOZ and TO-IFI16. The triple mutant herpes virus (TO) is replication-deficient due to the deletion of the essential ICP4, ICP27, and ICP22 genes, respectively. Vertical bars indicate deletions. The two recombinant vectors contain the lacZ and IFI116 transgene under the control of the HSV ICP0 promoter in the UL41 locus. (B) Time course of IFI16 expression after infection of HUVEC with TO-IFI16 vector or in control cells infected with TOZ as determined by Western blot analysis. Equal amounts of total cell extracts from HUVEC uninfected (lane 1), or infected with TOZ or TO-IFI16 vectors at 24 hpi (lanes 2 and 3), 48 hpi (lanes 4 and 5), or 72 hpi (lanes 6 and 7), respectively. The presence of IFI16 was detected with affinity-purified rabbit polyclonal monospecific Abs. Actin immunodetection with a monoclonal antibody (Boehringer) was performed as internal control. (C) Growth rates of TOZ- or TO-IFI16-infected HUVEC. Cells were seeded at equal densities in EGM2 plus 2% FBS (2.5×10^3 cells/cm^2), and at the indicated time points, cells were trypsinized, combined with any floating cells, pelleted, and counted with a hemocytometer. More than 200 cells were counted for each variable. Data are expressed as mean ± SD ($n = 3$).

protein reversibly inhibits HUVEC proliferation without causing cell death in accord to the results obtained with Ifi204 overexpression in mouse fibroblasts [19,20]. These conclusions are further supported by the finding that IFI16-expressing HUVEC marginally undergo apoptosis as shown by annexin V binding (data not shown).

Altogether, these results demonstrate that sustained and transient expression of exogenous IFI16 halts growth of proliferating HUVEC and hence that this system is suitable for in vitro angiogenesis studies.

Inhibition of HUVEC chemotaxis, invasion, and tube morphogenesis by IFI16 overexpression

Endothelial cell responses to angiogenic factors can be measured in vitro by assessment of induction of endothelial cell chemotaxis and chemoinvasion [33–36]. For this purpose, HUVECs were infected with either TO-IFI16 or TOZ viruses or left uninfected, and their migration and invasion capabilities evaluated. Infection of endothelial cells with TO-IFI16 inhibited chemoattractant-induced migration through gelatin-coated porous membranes by 54% compared to TOZ-infected cells whose migration degree is similar to that observed with uninfected endothelial cells. When both VEGF and bFGF were omitted in the lower chamber, no migration was observed (Fig. 3A). Because it has been demonstrated that IFNs inhibit endothelial cell migration across the basal lamina propria [4,5], we tested the effect of IFI16 expression on VEGF and bFGF-induced invasion (transmigration) of a reconstituted basal lamina in modified Boyden chambers. In this assay [35,36], cells transmigrate from an upper well through a porous filter coated with Matrigel toward chemoattractants (i.e. VEGF and bFGF) in the lower chamber. As shown in Fig. 3B, the presence of chemoattractants induced invasion of TOZ-infected-HUVEC through the Matrigel to a degree similar to that observed with uninfected HUVEC (95 ± 5 vs. 103 ± 6 cells/field, respectively). By contrast, overexpression of IFI16 reduced HUVEC migration by 49% as compared with TOZ virus. As shown before in the chemotaxis assay, when

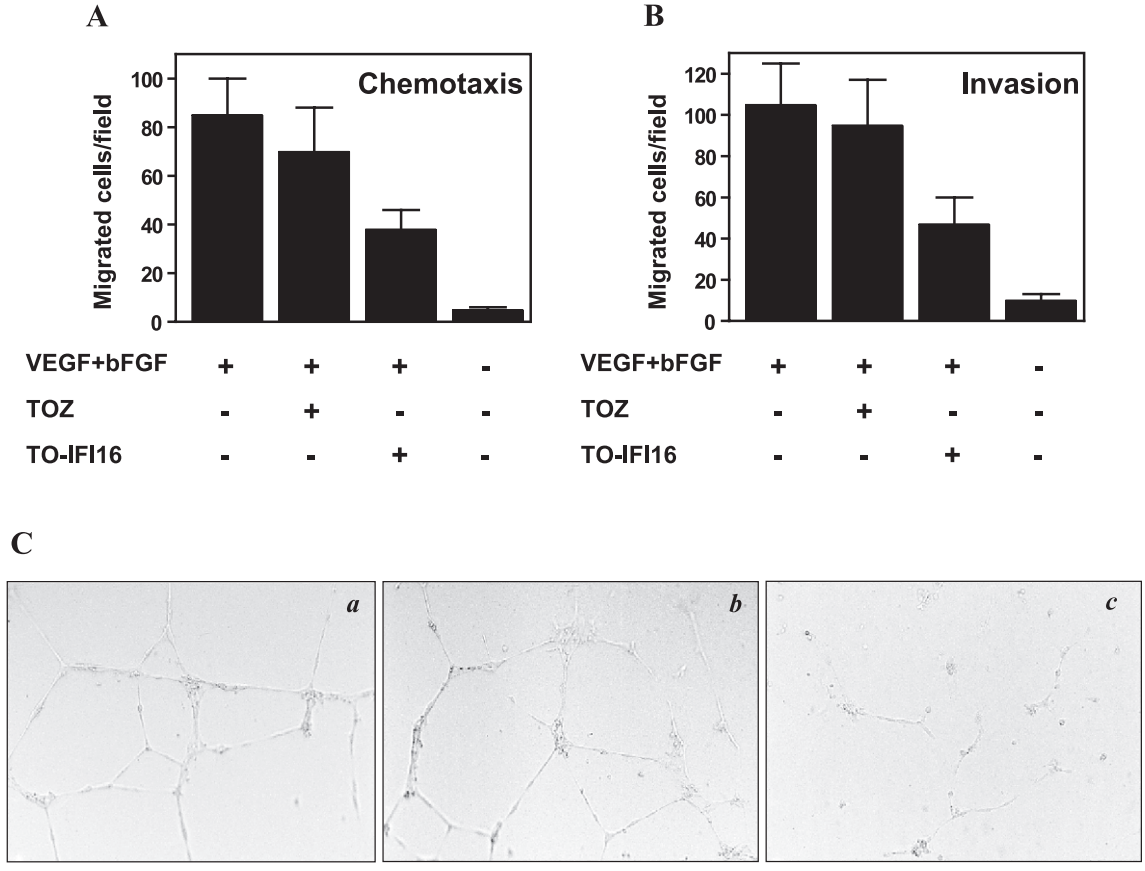

Fig. 3. Sustained IFI16 expression inversely correlates with HUVEC migration, invasion, and tube morphogenesis. (A,B) VEGF and bFGF-induced migration (A) and invasion (B) of HUVEC in modified Boyden chambers. Cells uninfected or infected with TOZ and TO-IFI16, respectively (36 hpi), were placed in the upper compartment of 24-well Boyden chambers as described in Materials and methods. VEGF and bFGF were added in lower wells. Cells migrated through the filter were counted after 6 h and data are expressed as the number of migrated cells in high-power fields. Data are expressed as mean ± SD ($n = 3$). (C) Tube Morphogenesis activity. Cells (8×10^4 cells/well) uninfected (a) or infected with TOZ (b) and TO-IFI16 (c), respectively (36 hpi), were seeded onto Matrigel-precoated wells and cultured in presence of complete EGM-2 medium. Photographs were taken 12 h later. Original magnification, ×160. Each experiment performed in triplicate has been repeated at least five times and one representative is reported.

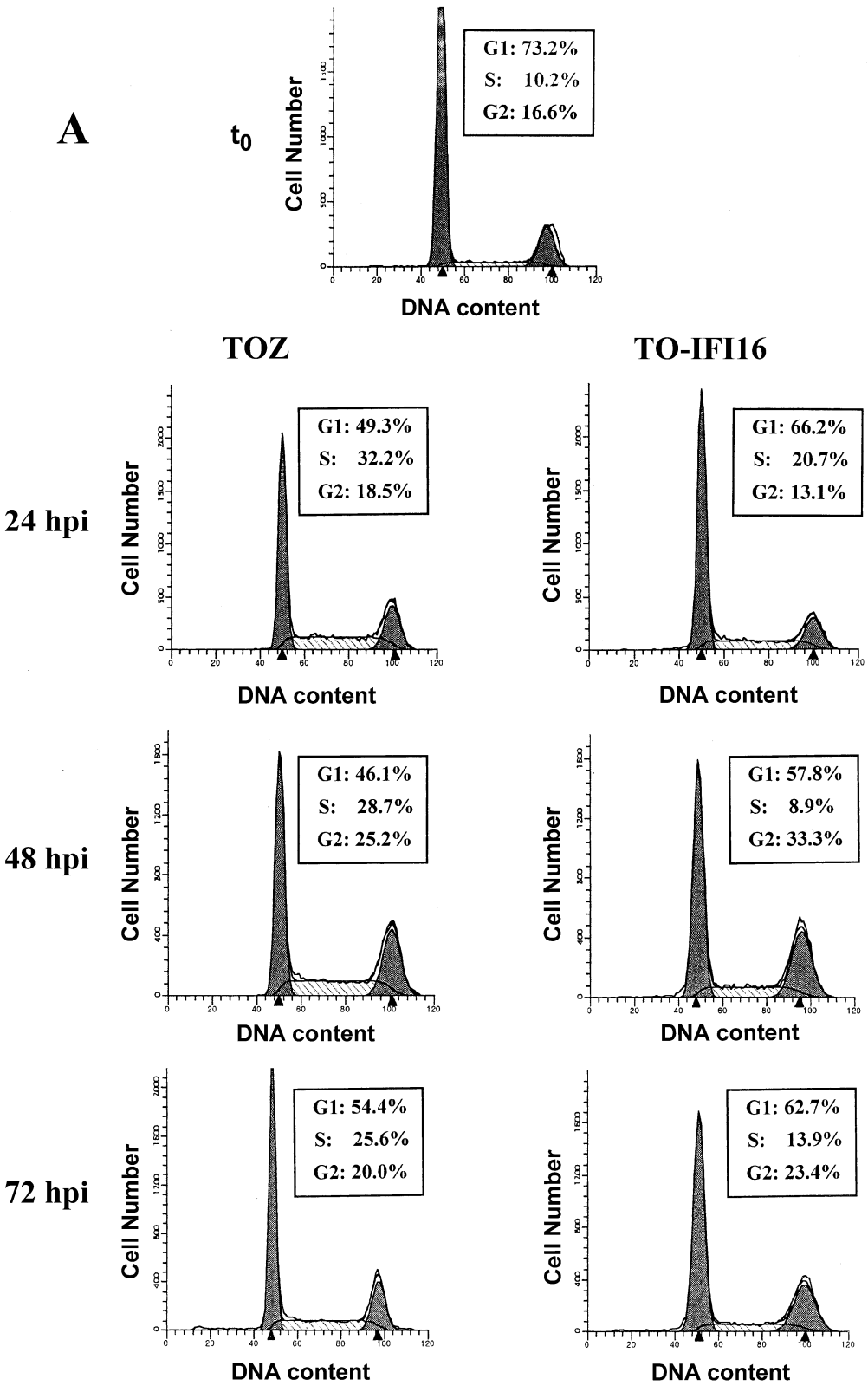

Fig. 4. Sustained IFI16 overexpression inhibits HUVEC cell cycle progression. (A) Growth-arrested HUVEC (indicated as t_0) were infected with TOZ or TO-IFI 16 vectors, replated at low cell density, and then cultured in complete EGM-2 medium. At the indicated times post infection, cell cycle distribution was evaluated. (B) Proliferating HUVEC (indicated as t_0) were infected with TOZ or TO-IFI16 vectors, replated at low cell density, and at the indicated times post infection analyzed for cell cycle distribution. Cellular DNA content was assessed with a FACScalibur flow cytometer (Becton and Dickinson) and analyzed with the ModFit LT software program (Becton and Dickinson). The experiments were repeated three times and one representative is reported.

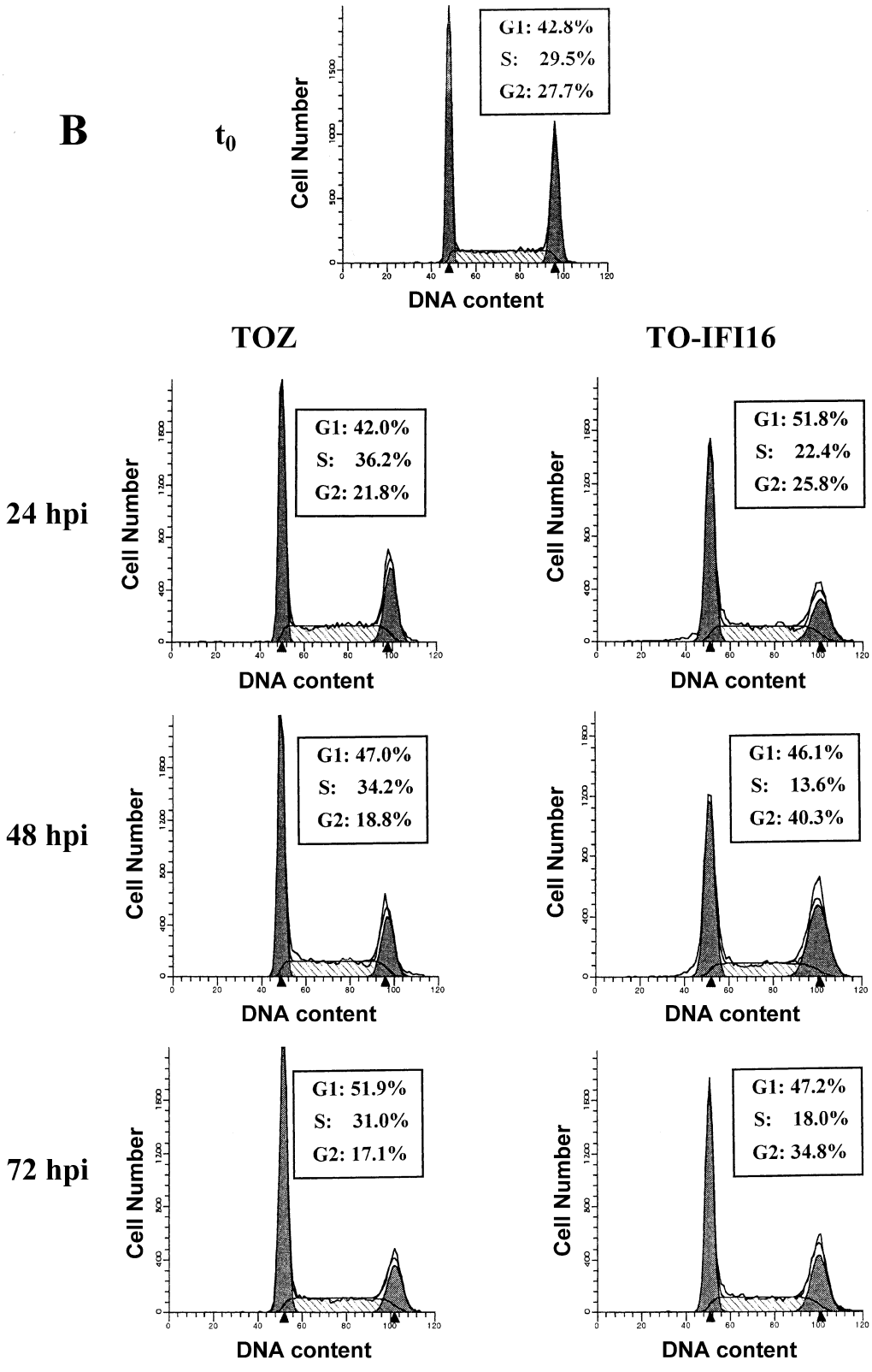

Fig. 4 (*continued*).

chemoattractants were not present, HUVEC migration through the Matrigel-coated membrane was not stimulated (Fig. 3B).

Apart from migration and invasion, tube formation is another important parameter of endothelial function that can be evaluated in vitro. HUVEC cultured on a Matrigel

rapidly align, extend processes into the matrix, and, finally, form capillary-like structures [37,38]. These structures are composed of polarized cells connected via complex junctions surrounding a central lumen. Within 24 h after seeding on Matrigel, TOZ-infected HUVEC showed the typical anastomosed cellular network observed with uninfected HUVEC, with an increased number of intercellular contacts and overall complexity of the network (Fig. 3C, insets a and b). In contrast, IFI16-overexpression completely inhibited the formation of these capillary structures, blocking HUVEC growth and tube morphogenesis on Matrigel (Fig. 3C, inset c). To prove specificity of IFI16-mediated antiangiogenic activity, infected HUVEC were also analyzed for class I MHC expression. As shown by FACS analysis, this cellular function was not affected by IFI16 overexpression (data not shown).

Altogether, these data demonstrate that sustained expression of IFI16 impairs some functions of HUVEC considered to be important in vitro parameters of angiogenesis.

Sustained IFI16 overexpression inhibits HUVEC cell cycle progression

We have previously shown that mouse 3T3 cells arrest in the G1 phase of the cell cycle upon transfection of the Ifi202 or Ifi204 genes [39,40]. This arrest was not further characterized, nor was the fate of the cells upon growth inhibition, that is senescence, apoptosis, or necrosis. To verify whether IFI16 causes a G1 arrest in HUVEC and determine its modalities, several experiments were performed using either HUVEC growth-arrested by both contact inhibition and culturing for 48 h in basal EBM-2 medium, or exponentially growing by culturing them at low density in EGM-2 medium.

Growth-arrested HUVEC (designated as t_0, Fig. 4A) were infected with TOZ or TO-IFI16 recombinant viruses, replated at low density in complete medium, and DNA content was determined by flow cytometry. Characterization at different intervals post infection provided a more complete picture of the life cycle kinetics of the infected cell lines. Fig. 4A shows the proportion of cell cycle arrest in infected cells at various time points post infection. After 24 h, about 51% of TOZ-infected cells had progressed to S and G2/M phases with only 49% in G1 phase. This pattern of cell distribution did not vary during the subsequent evaluations at 48 and 72 hpi, indicating that the empty vector does not influence cycle progression. In contrast, when HUVEC were infected with TO-IFI16, the highest proportion of cells remained in the G1 phase (66% cells at 24 h, >57% cells at 48 h, and >62% cells at 72 h), whereas the other phases displayed cell percentages significantly lower than those observed with TOZ-infected cells at all time points.

To determine whether the IFI16 activity on cell cycle progression depends on the phase of the cell cycle when the infection is performed, exponentially growing cells were infected with either TOZ and TO-IFI16 recombinant viruses, replated at low density in complete medium, and at various time points post infection the DNA content was analyzed. As shown in Fig. 4B, infection with TOZ vector did not significantly influence cell cycle progression from 24 to 72 hpi. Cell percentage in G1 increased from >42% to >51%, decreased from >21% to 17% in G2, and from 36% to 31% in S. A different pattern of cell distribution emerged with exponentially growing TO-IFI16-infected cells. At 24 h post infection, >51% HUVEC were in G1 phase, >25% in G2 phase, and >22% in S phase. At 48 h post infection, >46% HUVEC were in G1 phase, >13% in S phase, but, remarkably, >40% HUVEC accumulated in G2/M phase. Finally, at 72 h post infection, >47% HUVEC were in G1, about 18% in G2, and >34% were in S phase.

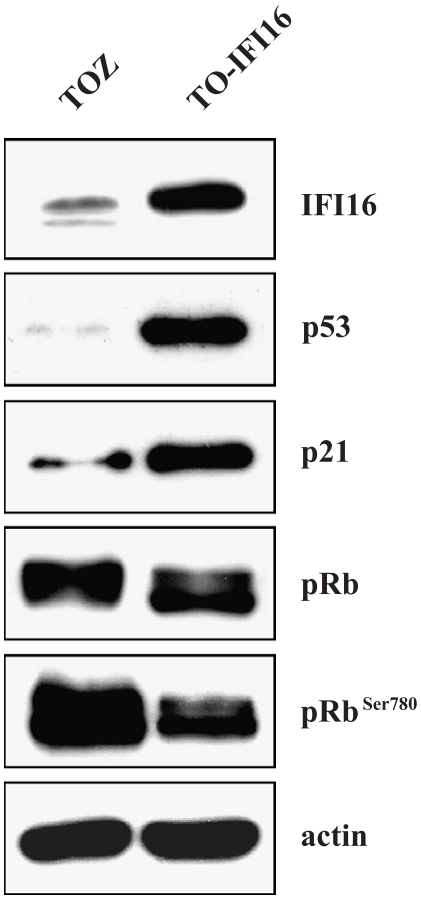

Fig. 5. Effect of IFI16 overexpression on cell cycle regulatory proteins. Immunoblots of cellular lysates corresponding to TOZ- or TO-IFI16-infected cells are shown. At 48 h after infection, cell lysates were prepared, and equal amounts (20 μg) were separated by gel electrophoresis and transferred to Immobilon membranes. The proteins were then probed with rabbit affinity-purified anti-IFI16, anti-p53, anti-p21, anti-pRb, and anti-ppRb Abs. The membrane was then incubated with the appropriate secondary Ab conjugated with horseradish peroxidase and visualized with an ECL kit (Amersham). Actin immunodetection was performed as an internal control.

Altogether, these results demonstrate that IFI16 gene inhibits the progression of HUVEC through the cell cycle, but the outcome of cell accumulation strictly depends on the growth phase in which IFI16 overexpression occurs. When it is overexpressed in growth-arrested cells, they do not enter the S phase and accumulate in G1, whereas if IFI16 gene is overexpressed in an exponentially growing population, they accumulate in the G2/M phase.

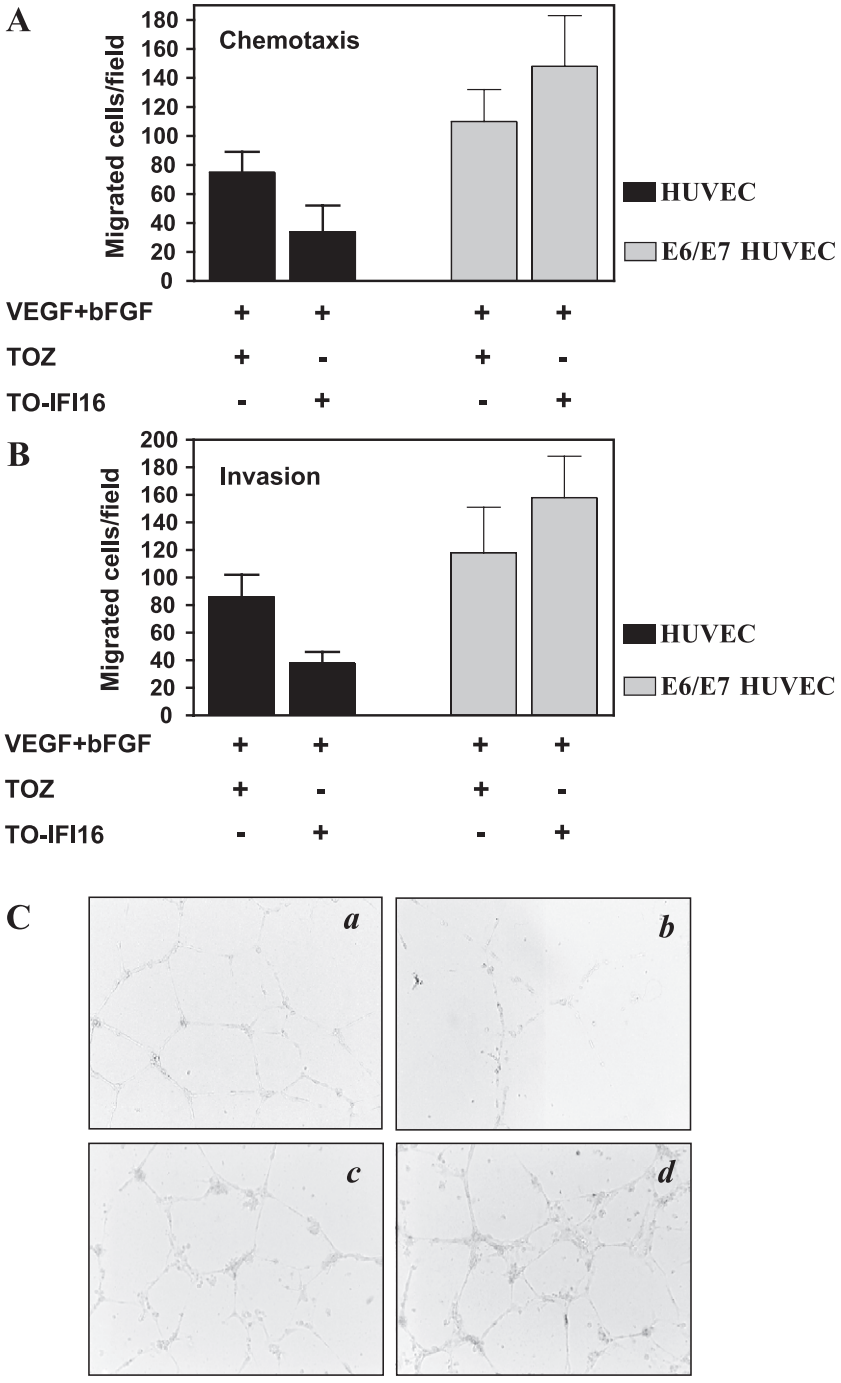

Fig. 6. HPV16 E6/E7 oncogenes reverse the effects of IFI16 overexpression on HUVEC migration, invasion and tube morphogenesis. (A,B) VEGF and bFGF-induced migration (A) and invasion (B) of primary or HPV16 E6/E7 immortalized HUVEC in modified Boyden chambers. Cells infected with TOZ and TO-IFI16, respectively (36 hpi) were placed in the upper compartment of 24-well Boyden chambers as described in Materials and methods. VEGF and bFGF were added in lower wells. Cells migrated through the filter were counted after 6 h and data are expressed as the number of migrated cells in high-power fields. Data are expressed as mean ± SD ($n = 3$). (C) Morphogenesis activity. Primary or HPV16 E6/E7 immortalized HUVEC (8×10^4 cells/well) infected with TOZ (a and c, respectively) or TO-IFI16 (b and d, respectively) (36 hpi) were seeded onto Matrigel-precoated wells and cultured in presence of complete EGM-2 medium. Photographs were taken 12 h later. Original magnification, ×160. Each experiment performed in triplicate was repeated at least three times and one representative is reported.

Earlier reports showed that 200 gene families modulate cell growth by interacting with both p53 and pRb systems and down-regulate transcription mediated by E2F [20,22,40]. To further define the molecular events underlying the effects of IFI16 on HUVEC physiology, that is migration, invasion, tube formation, and proliferation, the steady state levels of the tumor suppressor proteins p53 and pRb, and the p21Cip1/WAF1 (p21WAF1), were monitored at 48 h after infection with either TO-IFI16 or TOZ recombinant viruses, when cell growth is arrested according to FACS analysis. As shown in Fig. 5, the levels of both p53 and p21WAF1 were significantly augmented upon infection with TO-IFI16 compared to those observed with the TOZ virus. Interestingly, the increase in p21WAF1 suggest that the induced p53 is functional [41]. When the levels of pRb expression were analyzed, although no modulation of the Rb steady state levels was observed, the protein appeared to be significantly hypophosphorylated, suggesting that it is in the active form typical of cells arrested in the G1 phase.

Inhibition of cell cycle progression by IFI16 overexpression is counteracted by HPV16 E6/E7 genes

The best characterized HPV16 E6 activity is its ability to induce degradation of the tumor suppressor protein p53 via the ubiquitin pathway [42,43]. The other viral oncoprotein, E7, from the high-risk HPV types, is a strong activator of the cell cycle and promotes G1/S transition, even in the presence of negative cell cycle regulators [44]. This E7 activity is in part explained by inactivation of the tumor suppressor retinoblastoma [44].

To establish whether IFI16 antiangiogenic activity requires both functional p53 and pRb pathways, HUVEC were transduced with recombinant retroviruses expressing the E6 and E7 genes of HPV16. E6 and E7 gene expression was confirmed by RT-PCR (data not shown). Transduced HUVEC were then infected with both TO-IFI16 and TOZ and the ability of E6/E7 proteins to alleviate the in vitro activity of IFI16 on HUVEC functions was determined.

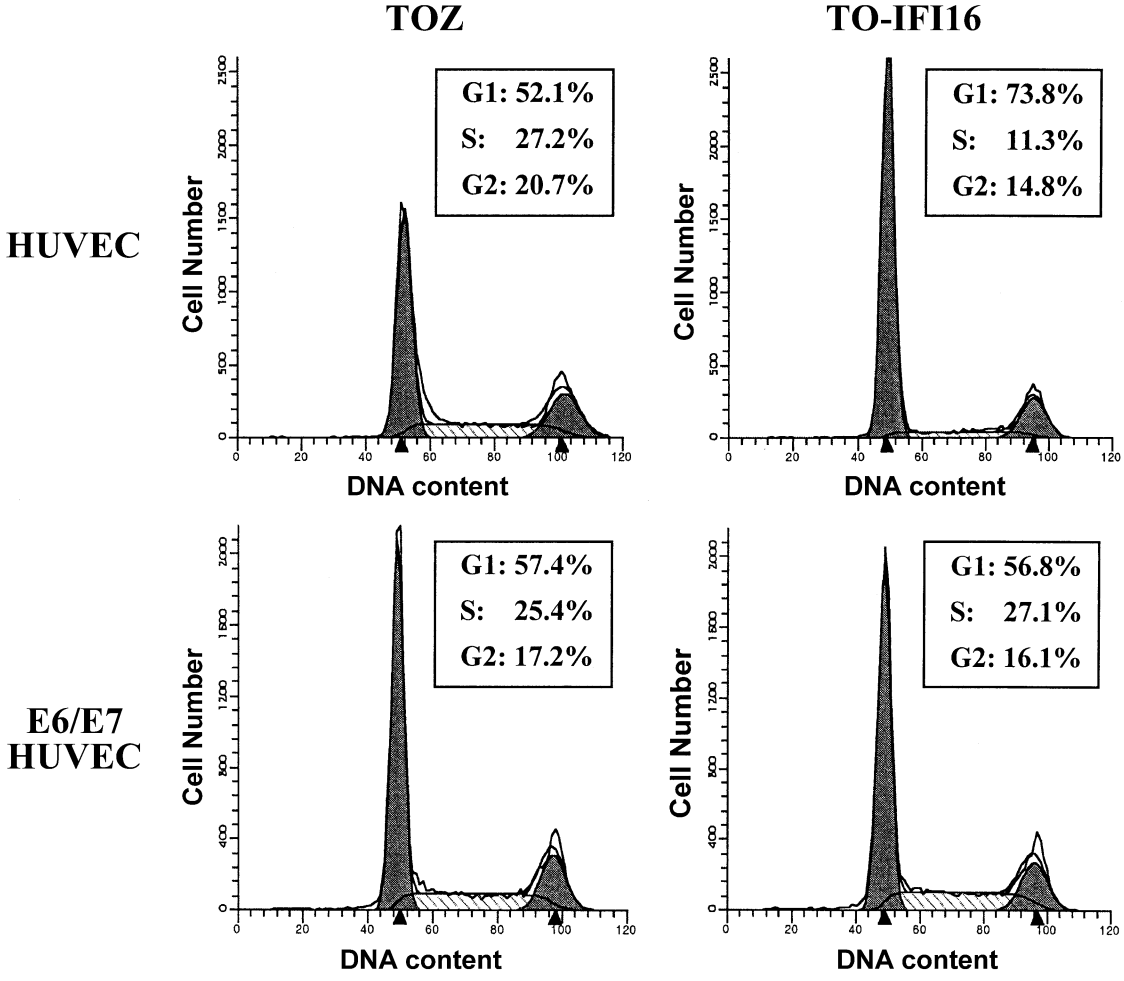

Fig. 7. HPV16 E6/E7 oncogenes reverse the effects of IFI16 overexpression on HUVEC cell cycle progression. Growth-arrested primary or HPV16 E6/E7-immortalized HUVEC were infected with TOZ or TO-IFI16 vectors, replated at low cell density, and then cultured in complete EGM 2 medium. At 48 hpi, cell cycle distribution was evaluated. Cellular DNA content was assessed with a FACScalibur flow cytometer (Becton and Dickinson) and analyzed with the ModFit LT software program (Becton and Dickinson). The experiments have been repeated three times and one representative is reported.

For this purpose, parental- or E6/E7 immortalized-HUVEC were infected with TOZ or TO-IFI16 and their motility and invasion capabilities, tube morphogenesis, and cycle progression compared. As shown in Fig. 6, infection with TO-IFI16 strongly inhibited motility (panel A) and invasion capabilities (panel B) along with the formation of capillary-like structures (panel C) of primary HUVEC compared with TOZ-infected HUVEC. In contrast, when HUVEC immortalized with HPV16 E6/E7 oncogenes were infected with TO-IFI16, the number of cells migrating throughout the filters coated with gelatin (148 ± 16 migrating cells/field) or Matrigel (158 ± 15 invading cells/field) was significantly higher than that observed with cells infected with TOZ (110 ± 8 migrating cells/field and 118 ± 12 invading cells/field, respectively). In line with these results, IFI16 overexpression in immortalized HUVEC significantly enhanced tube formation with an increased number of intercellular contacts and overall complexity of the network compared to that observed with immortalized HUVEC infected with TOZ (Fig. 6C, insets c and d vs. a and b, respectively).

To determine whether HPV16 E6/E7 oncogenes reverse IFI16-induced growth inhibition, parental HUVEC or HUVEC transduced with pBabeE6/E7 (E6/E7 HUVEC) were growth-arrested both by contact inhibition and by culturing them in EBM-2 medium; cells were then infected with TOZ or TO-IFI16, and at 48 hpi the cell cycle profiles were determined by FACS analysis. As shown in Fig. 7, E6/E7 HUVEC overexpressing IFI16 displayed a much lower percentage of cells in G1 than that observed with primary HUVEC infected with TO-IFI16 (56.8% vs. 73.8%, respectively), but very similar to that observed with E6/E7 HUVEC or primary HUVEC infected with TOZ. In contrast, an opposite effect was observed when the other phases of the cell cycle were compared: a higher percentage of cells in both S and G2/M was constantly observed in E6/E7 HUVEC similar to those observed with cells infected with TOZ.

Altogether, these results suggest that in the absence of functional p53 and pRb systems following E6/E7 infection, IFI16 not only loses its ability to exert antiangiogenic and antiproliferative activities, but even enhances some parameters of in vivo angiogenesis, that is endothelial cell invasion and tube morphogenesis.

Discussion

Earlier reports demonstrated that the mouse Ifi200 genes, namely Ifi202 and Ifi204, when overexpressed in primary mouse embryo fibroblasts or NIH3T3 cells, arrest their proliferation by delaying transition from G1 to S phase [39,40]. Interaction with both pRb and p53 systems appears to be essential for this antiproliferative activity [19–23,45]. By contrast, less information is available about the human homolog IFI16, probably due to the lack of an appropriate normal cellular model in the human system.

In this study, we have developed a suitable experimental model to test IFI16 biological functions by using primary HUVEC, which are usually poorly transfectable by conventional methods, transduced with a HSV-derived replication-defective vector carrying the IFI16 cDNA. The choice of the endothelial cell system was dictated by two previous findings. In vivo, along with hematopoietic and stratified squamous epithelial cells, endothelial cells specifically express IFI16, suggesting a role of this gene in the control of their physiology. In vitro, Western blotting analysis demonstrated that in proliferating HUVEC, IFI16 expression is barely detectable and gradually increases when cell growth halts upon reaching confluence. It may thus be involved in the modulation of endothelium differentiation and proliferation. The use of the HSV-derived TO-IFI16 vector allowed overexpression of the IFI16 protein in primary HUVEC and revealed for the first time that sustained IFI16 expression suppresses their growth, migration, and organization into capillary-like structures, together with cell cycle progression. Taken together, our results suggest that IFI16 contributes to maintenance of a quiescent, differentiated phenotype in HUVEC and that its expression must decrease for tube morphogenesis to proceed.

Angiogenesis occurs by a series of sequential steps. In response to angiogenic stimuli, endothelial cells degrade the basement membrane by secreting proteolytic enzymes that include metalloproteinases (MMPs) and serine proteases [1,2,37]. The cells then migrate through the degraded basement membrane and continue to break down the interstitial stroma as they move. The endothelial cells at the tip of sprout do not usually divide, whereas the trailing cells at the base of the new vessel proliferate [38]. The endothelium then aligns in a bipolar fashion to form a lumen. Given the crucial function of MMPs in the degradation of basement membrane in the initial steps of angiogenesis, it is therefore conceivable that one of the mechanisms exploited by IFI16 to inhibit chemotaxis, chemoinvasion, and tube morphogenesis is down-regulation of MMPs secretion. We have, in fact, observed that in zymography experiments the supernatants from HUVEC infected with TO-IFI16 contain less proteolytic activity attributable to MMP2 and MMP9 in consequence of a decreased expression of MMP2 and MMP9 proteins (data not shown). This observation is consistent with a previous report showing that another IFN-inducible gene, namely the guanylate protein-1 GTPase, controls the invasive and angiogenic capability of endothelial cells through inhibition of MMP-1 expression [10].

In addition to proteolytic enzyme secretion and migration, tube morphogenesis depends on endothelial cell proliferation [1,2,37,38]. Analysis of cell growth and cell cycle profile upon TO-IFI16 infection suggests that sustained expression of IFI16 affects HUVEC proliferation. Moreover, Western blotting analysis and IFI16 overexpression in

HPV16E6/E7-transduced cells revealed that its activity depends on both functional p53 and pRb pathways. The p53 and pRb protein families are key cell cycle regulators that manage the response to a variety of stimuli either by inducing cell growth arrest, senescence, or apoptosis [46–48]. The mouse homolog p202 was found to bind the murine homolog of the human p53-binding protein 1 (p53BP1) and regulate transcriptional activation mediated by p53 [45]. The mouse p204 contains the pRb binding motifs LXCXE and binds pRb [20]. Its overexpression, as here with IFI16, delays progression of cells from the G1 to the S phase. IFI16 directly binds to the C-terminal region of p53 through the consensus motif MFHATVAT in the 200-amino-acid domain a, and augments p53-mediated transcriptional activation [23]. The outcome of immunoblotting analysis confirms that sustained IFI16 expression increases both p53 and pRb levels, the latter in its hyposphorylated form. The molecular mechanisms underlying cell cycle regulation by p53 have been well defined. p53 transcriptionally up-regulates the p21WAF1 gene, the protein product of which inhibits the kinase activity of cdk4/cyclin D [49]. Activation of cdk4/cyclin D results in phosphorylation of pRb, release of pRb from the pRb/E2F/DP-1 complex, and progression to S phase via activation of E2F/DP-1 responsive genes [50]. Thus, p21WAF1 provides a link between IFI16, p53, and pRb regulatory pathways. It can act to limit the phosphorylation of pRb, thereby preventing cells from exiting the G1 phase of the cell cycle.

The transforming proteins of DNA tumor viruses such as SV40 large T antigen, adenovirus E1A/E1B, or HPV16 E6/E7 extend the life span of human cells in culture [51]. Extension of life span is dependent on the ability of these viral proteins to target the tumor suppressor proteins, p53 and pRb, and render them functionally inactive. When HPV16 E6/E7-transduced HUVEC were analyzed to determine their tubulogenesis activity and cell cycle progression upon IFI16 overexpression, it became evident that inactivation of both p53 and pRb pathways renders them resistant to IFI16 antitubulogenesis and antiproliferative activities. In this context, Xin et al. [52] reported that ectopic expression of IFI16 in prostate cancer cell lines resulted in colony formation inhibition that differed with respect to expression of functional pRb and p53; the maximum inhibition was seen in LNCaP (these cells express functional Rb) and minimum inhibition was seen in DU-145 cells (these cells do not express functional Rb and p53). Importantly, up-regulation of p21WAF1 and inhibition of E2F-stimulated transcription accompanied inhibition of cell growth by IFI16 in these prostate cancer cell lines. Moreover, Johnstone et al. [23] earlier reported that IFI16 can directly bind to the C-terminal region of p53 and augment p53-mediated transcriptional activation of a reporter construct containing the promoter from the p21WAF1 gene with a p53-binding site. Altogether, these observations supported the possibility that IFI16-mediated antiangiogenic activity depends on the presence of functional p53 and pRb. On the contrary, Kwak et al. [53] reported that the inhibition of endogenous IFI16 expression by small interfering RNA (siRNA) induces p21WAF1 mRNA and protein expression through p53, and results in cell cycle arrest. However, there are numerous differences between the experiments conducted by Kwak et al. and the ones reported here that may affect the cellular response to growth-inhibitory signals. For example, they have employed a tumor cell line, U2OS, expressing high level of endogenous IFI16, whereas we have used primary normal endothelial cells (HUVEC) whose basal IFI16 level is very low and highly inducible by various stimuli. In addition, unlike our experiments, they have inhibited endogenous IFI16 expression in U2OS cells that constitutively display high IFI16 levels and strongly argues against its antiproliferative activity. In light of this, IFI16 is possibly functionally inactive in U2OS, or it may even be the case that mutations occurred in its downstream signaling pathways.

Our observations on the capability of IFI16 to control some aspects of endothelial cell physiology have some interesting implications. The first is that until now, it has been difficult to assign a biological function to the IFI16 gene. Its homology to the mouse Ifi204 indicated its involvement in cell cycle control, but the lack of efficient transducing vectors and appropriate cell systems has hampered definition of its biological function. HSV-derived vectors overcame these obstacles and provided the first evidence of a link between IFI16 and inhibition of cell proliferation. The second is based on previous in vivo findings. Immunohistochemistry revealed that IFI16 is highly expressed in endothelial and epithelial cells and may be of significance in their physiology. The use of primary HUVEC established a link between IFI16 expression and control of tube morphogenesis in vitro, considered to be the counterpart of in vivo angiogenesis. The third implication is that at the molecular level IFI16 exploits both p53 and pRb pathways to control the cell cycle and proliferation. Thus, these data may help to explain why in vivo transformed cells bearing mutations at these two important regulators of cell cycle progression become resistant to the IFN treatment because of the acquisition to evade the IFN antiproliferative and antiangiogenic activities. The fourth one is that IFNs so far have been found to have antiangiogenic properties in vivo and in vitro through down-regulation of the expression of proangiogenic molecules, such as bFGF [6], MMP-2 and MMP-9 [7–9], and IL-8 [10]. Our present findings showing that sustained expression of IFI16 impairs tube morphogenesis and growth by inhibiting HUVEC cell cycle progression provide a further illustration of the molecular mechanisms exploited by IFNs to regulate angiogenesis.

Acknowledgments

We thank Filippo Renò (Novara) and Adriana Albini (Genova) for helpful discussion and manuscript revision,

and Barbara Azzimonti (Novara) for preparing retroviral vectors. We thank Joseph Trapani for his generous gift of the pBKS-IFI16 plasmid. This work was supported by grants from Associazione Italiana per la Ricerca sul Cancro, Special Project Oncology "Compagnia di San Paolo"/ FIRMS, Lega Italiana per la Lotta contro i Tumori (section of Novara) and Program 40% (MIUR).

References

[1] W. Risau, Mechanisms of angiogenesis, Nature 386 (1997) 671–674.
[2] G.D. Yancopoulos, S. Davis, N.W. Gale, J.S. Rudge, S.J. Wiegand, J. Holash, Vascular-specific growth factors and blood vessel formation, Nature 407 (2000) 242–248.
[3] R. Kerbel, J. Folkman, Clinical translation of angiogenesis inhibitors, Nat. Cancer Rev. 2 (2002) 727–738.
[4] M. Iurlaro, R. Benelli, L. Masiello, M. Rosso, A. Albini, Beta interferon inhibits HIV-1 Tat induced angiogenesis: synergism with 13-cis retinoic acid, Eur. J. Cancer 34 (1998) 570–576.
[5] A. Albini, C. Marchisone, F. Del Grosso, R. Benelli, L. Masiello, L. Tacchetti, M. Bono, M. Ferrantini, C. Rozera, M. Truini, F. Belardelli, L. Santi, D.M. Noonan, Inhibition of angiogenesis and vascular tumor growth by interferon-producing cells, Am. J. Pathol. 156 (2000) 1381–1393.
[6] E. Guenzi, K. Topolt, E. Cornali, C. Lubeseder-Martellato, A. Jorg, K. Matzen, C. Zietz, E. Kremmer, F. Nappi, M. Schwemmle, C. Hohenadl, G. Barillari, E. Tschachler, P. Monini, B. Ensoli, M. Sturzl, The helical domain of GBP-1 mediates the inhibition of endothelial cell proliferation by inflammatory cytokines, EMBO J. 20 (2001) 5568–5577.
[7] R.K. Singh, M. Gutman, C.D. Bucana, R. Sanchez, N. Llansa, I.J. Fidler, Interferon alpha and beta down-regulate the expression of basic fibroblast growth factor in human carcinomas, Proc. Natl. Acad. Sci. U. S. A. 92 (1995) 4562–4566.
[8] K. Gohji, I.J. Fidler, R. Tsan, R. Radinsky, A.C. van Eshenbach, T. Tsuruo, M. Nakajima, Human recombinant interferons-beta and -gamma decrease production and invasion by human KG-2 renal carcinoma cells, Int. J. Cancer 58 (1994) 380–384.
[9] N. Kato, A. Nawa, K. Tamakoshi, F. Kikkawa, N. Suganuma, T. Okamoto, S. Goto, Y. Tomoda, M. Hamaguchi, M. Nakajima, Suppression of gelatinase production with decreased invasiveness of choriocarcinoma cells by recombinant interferon-β, Am. J. Obstet. Gynecol. 172 (1995) 601–606.
[10] E. Guenzi, K. Topolt, C. Lubeseder-Martellaro, A. Jorg, E. Naschberger, A. Albini, M. Sturzl, The guanylate binding protein-1 GTPase controls the invasive and angiogenic capability of endothelial cells through inhibition of MMP-1 expression, EMBO J. 22 (2003) 3772–3782.
[11] R.K. Singh, M. Gutman, N. Llansa, I.J. Fidler, Interferon-β prevents the upregulation of interleukin-8 in human melanoma cells, J. Interferon Cytokine Res. 16 (1996) 577–584.
[12] G.R. Stark, I.M. Kerr, B.R. Williams, R.H. Silverman, R.D. Schreiber, How cells respond to interferons, Annu. Rev. Biochem. 67 (1998) 227–264.
[13] P. Lengyel, D. Choubey, S.J. Li, B. Datta, The interferon-activatable gene 200 cluster: from structure toward function, Semin. Virol. 6 (1995) 203–215.
[14] S. Landolfo, M. Gariglio, G. Gribaudo, D. Lembo, The Ifi 200 genes: an emerging family of IFN-inducible genes, Biochimie 80 (1998) 721–728.
[15] R.W. Johnstone, J.A. Trapani, Transcription and growth regulatory functions of the HIN-200 family of proteins, Mol. Cell. Biol. 19 (1999) 5833–5838.
[16] J.A. Trapani, K.A. Browne, M.J. Dawson, R.G. Ramsay, R.L. Eddy, T.B. Show, P.C. White, B. Dupont, A novel gene constitutively expressed in human lymphoid cells is inducible with interferon-γ in myeloid cells, Immunogenetics 19 (1992) 369–376.
[17] G.R. Burrus, J.A. Briggs, R.C. Briggs, Characterization of the human myeloid cell nuclear differentiation antigen: relationship to interferon-induced proteins, J. Cell. Biochem. 48 (1992) 190–202.
[18] K.L. DeYoung, M.E. Ray, Y.A. Su, S.L. Anzick, R.W. Johnstone, J.A. Trapani, P.S. Meltzer, J.M. Trent, Cloning of a novel member of the human interferon-inducible gene family associated with control of tumorigenicity in a model of human melanoma, Oncogene 15 (1997) 453–457.
[19] M. Lembo, C. Sacchi, C. Zappador, G. Bellomo, M. Gaboli, P.P. Pandolfi, M. Gariglio, S. Landolfo, Inhibition of cell proliferation by the interferon-inducible 204 gene, a member of the Ifi 200 cluster, Oncogene 16 (1998) 1543–1551.
[20] L. Hertel, S. Rolle, M. De Andrea, B. Azzimonti, R. Osello, G. Gribaudo, M. Gariglio, S. Landolfo, The retinoblastoma protein is an essential mediator that links the interferon-inducible 204 gene to cell-cycle regulation, Oncogene 19 (2000) 3598–3608.
[21] M. De Andrea, M. Ravotto, E. Noris, G.-G. Ying, D. Gioia, B. Azzimonti, M. Gariglio, S. Landolfo, The interferon-inducible gene, Ifi204, acquires malignant transformation capability upon mutation at the Rb-binding sites, FEBS Lett. 515 (2002) 51–57.
[22] C.-J. Liu, B. Ding, H. Wang, P. Lengyel, The MyoD-inducible p204 protein overcomes the inhibition of myoblasts differentiation by Id proteins, Mol. Cell. Biol. 22 (2002) 2893–2905.
[23] R.W. Johnstone, W. Wei, A. Greenway, J.A. Trapani, Functional interaction between p53 and the interferon-inducible nucleoprotein IFI16, Oncogene 19 (2000) 6033–6042.
[24] H. Xin, S. D'Souza, L. Fang, P. Lengyel, D. Choubey, p202, an interferon-inducible negative regulator of cell growth, is a target of the adenovirus E1A protein, Oncogene 20 (2001) 6828–6839.
[25] J.Y. Mori, A. Rashid, B.A. Leggett, J. Young, L. Simms, P.M. Kuehl, P. Langenberg, S.J. Meltzer, O.C. Stine, Instabilotyping: comprehensive identification of frameshift mutations caused by coding region microsatellite instability, Cancer Res. 61 (2001) 6046–6049.
[26] S. Varambally, S.M. Dhanasekaram, M. Zhou, T.R. Barrette, C. Kumar-Sinha, M.G. Sanda, D. Ghosh, K.J. Pienta, R.G. Sewalt, A.P. Otte, M.A. Rubin, A.M. Chinnaiyan, The polycomb group protein EZH2 is involved in progression of prostate cancer, Nature 419 (2002) 624–629.
[27] H. Xin, J. Curry, R.W. Johnstone, B.J. Nickoloff, D. Choubey, Role of IFI16, a member of the interferon-inducible p200-protein family, in prostate epithelial cellular senescence, Oncogene 22 (31) (2003) 4831–4840.
[28] M. Gariglio, B. Azzimonti, M. Pagano, G. Palestro, M. De Andrea, G. Valente, G. Voglino, L. Navino, S. Landolfo, Immunohistochemical expression analysis of the human interferon-inducible gene IFI16, a member of the HIN200 family, not restricted to hematopoietic cells, J. Interferon Cytokine Res. 22 (2002) 815–821.
[29] W. Wei, C.J. Clarke, G.R. Somers, K.S. Cresswell, K.A. Loveland, J.A. Trapani, R.W. Johnstone, Expression of IFI16 in epithelial cells and lymphoid tissues, Histochem. Cell Biol. 119 (2003) 45–54.
[30] D.M. Krisky, P.C. Marconi, T.J. Oligino, R.J. Rouse, D.J. Fink, J.B. Cohen, S.L. Watkins, J.C. Glorioso, Development of herpes simplex virus replication-defective multigene vectors for combination gene therapy application, Gene Ther. 5 (1998) 1517–1530.
[31] P. Marconi, M. Simonato, S. Zucchini, G. Bregola, R. Argnani, D. Krisky, J.C. Glorioso, R. Manservigi, Replication-defective herpes simplex virus vectors for neurotrophic factor gene transfer in vitro and in vivo, Gene Ther. 6 (1999) 904–912.
[32] W.S. Pear, G.P. Nolan, M.L. Scott, D. Baltimore, Production of high-titer helper-free retroviruses by transient transfection, Proc. Natl. Acad. Sci. U. S. A. 90 (1993) 8392–8396.
[33] A. Albini, Y. Iwamato, H.K. Kleinman, G.R. Martin, S.A. Aaronson, J.M. Kozlowski, R.N. McEwan, A rapid in vitro assay for quantitat-

ing the invasive potential of tumor cells, Cancer Res. 47 (1987) 3239–3245.
[34] G. Taraboletti, D. Roberts, L.A. Lotta, R. Giavazzi, Platelet thrombospondin modulates endothelial cell adhesion, motility and growth: a potential angiogenesis regulatory factor, J. Cell Biol. 111 (1990) 765–772.
[35] Y. Kubota, H.K. Kleinman, G.R. Martin, T.J. Lawley, Role of laminin and basement membrane in the morphological differentiation of human endothelial cells into capillary-like structures, J. Cell Biol. 107 (1988) 1589–1598.
[36] A. Albini, Tumor and endothelial cell invasion of basement membranes, Pathol. Oncol. Res. 14 (1998) 1–12.
[37] M. Nguyen, J. Arkell, J.C. Jackson, Human endothelial gelatinases and angiogenesis, Int. J. Biochem. Cell Biol. 33 (2001) 960–970.
[38] B. Lubarsky, M.A. Krasnow, Tube morphogenesis: making and shaping biological tubes, Cell 112 (2003) 19–28.
[39] D. Lembo, A. Angeretti, S. Benefazio, L. Hertel, M. Gariglio, F. Novelli, S. Landolfo, Constitutive expression of the interferon-inducible protein p202 in NIH 3T3 cells affects cell cycle progression, J. Biol. Regul. Homeostatic Agents 9 (1995) 42–46.
[40] G. Gribaudo, L. Riera, M. De Andrea, S. Landolfo, The antiproliferative activity of the murine interferon-inducible Ifi200 proteins depends on the presence of two 200 amino acid domains, FEBS Lett. 456 (1999) 31–36.
[41] K.F. Macleod, N. Sherry, G. Hannon, D. Beach, T. Tokino, K. Kinzler, B. Vogelstein, T. Jacks, p53-Dependent and independent expression of p21 during cell growth, differentiation, and DNA damage, Genes Dev. 9 (1995) 935–944.
[42] M. Thomas, D. Pim, L. Banks, The role of the E6-p53 interaction in the molecular pathogenesis of HPV, Oncogene 18 (1999) 7690–7700.
[43] M. Tommasino, R. Accardi, S. Caldeira, W. Dong, I. Malanchi, A. Smet, I. Zehbe, The role of TP53 in cervical carcinogenesis, Hum. Mutat. 21 (2003) 307–312.
[44] H. Zur Hausen, Papillomavirus causing cancer: evasion from host-cell control in early events in carcinogenesis, J. Natl. Cancer Inst. 78 (2000) 1–29.
[45] B. Datta, B. Li, D. Choubey, G. Nallur, P. Lengyel, p202, an interferon-inducible modulator of transcription, inhibits transcriptional activation by the p53 tumor suppressor protein, and a segment from the p53-binding protein 1 that binds to p202 overcomes this inhibition, J. Biol. Chem. 271 (1996) 27544–27555.
[46] A.J. Levine, p53, the cellular gatekeeper for growth and division, Cell 88 (1997) 323–331.
[47] C.H. Arrowsmith, Structure and function in the p53 family, Cell Death Differ. 6 (1999) 1169–1173.
[48] N. Dyson, The regulation of E2F by pRB-family proteins, Genes Dev. 12 (1998) 2245–2262.
[49] M.G. Ritt, J. Mayor, J. Wojcieszyn, R. Smith, C. Barton, J.F. Modiano, Sustained nuclear localization of p21/WAF-1 upon growth arrest induced by contact inhibition, Cancer Lett. 158 (2000) 73–84.
[50] G. Mulligan, T. Jacks, The retinoblastoma gene family: cousins with overlapping interests, Trends Genet. 14 (1998) 223–229.
[51] S.J. Flint, L.W. Enquist, R.M. Krug, V.R. Racaniello, A.M. Skalka (Eds.), Principles of Virology. Molecular Biology, Pathogenesis, and Control, ASM Press, Washington, DC, 2000.
[52] H. Xin, J. Curry, R.W. Johnstone, B.J. Nickoloff, D. Choubey, Role of IFI16, a member of the interferon-inducible p200-protein family, in prostate epithelial cellular senescence, Oncogene 22 (2003) 4831–4840.
[53] J.C. Kwak, P.P. Ongusaha, T. Ouchi, S.W. Lee, IFI16 as a negative regulator in the regulation of p53 and p21Waf1, J. Biol. Chem. 278 (2003) 40899–40904.